## Supporting information

# Achieving metal-free phosphorescence in dilutesolutions for imaging hypoxia in cells and tumors

Peng Li, § [a] Yurong Guo, § [b] Yan Jia, § [c] Hongwei Guan, [a] Chao Wang, [b] Zibo Wu, [b] Shuqing Sun, [b] Zongjin Qu, [a] Panwang Zhou,* [a] Guangjiu Zhao* [b]

[a] Institute of Molecular Sciences and Engineering, Shandong University, Qingdao 266237, China. E-mail: pwzhou@sdu.edu.cn

[b] Tianjin Key Laboratory of Molecular Optoelectronic Sciences, Department of Chemistry, School of Science, Tianjin University, Tianjin 300354, China. E-mail: gjzhao@tju.edu.cn

[c] State Key Laboratory of Molecular Reaction Dynamics, Dalian Institute of Chemical Physics, Chinese Academy of Sciences, Dalian 116023, China.

§ These authors contributed equally.

## Contents

### Part Ⅰ: Experimental and Theoretical Methods



### Part Ⅱ: Schemes, Equations, Tables and Figures

## Part Ⅰ: Experimental and Theoretical Methods

### 1. The characterization of the compounds

**1.1 General information:** All chemicals were used as received. Silica gel for column chromatography was 200-300 mesh. $^{1}H$ NMR (400 MHz), $^{13}C$ NMR (100 MHz), and $^{77}Se$ NMR spectra were recorded on Brüker Avance spectrometers. Chemical shifts are given in ppm (δ) and are referenced to those of Me4Si for $^{1}H$ NMR and $^{13}C$ NMR, and dipheny diselenide for $^{77}Se$ NMR. Multiplicities are declared as follow: s (singlet), bs (broad singlet), d (doublet), t (triplet), m (multiplet). High-resolution mass spectrometry (HRMS) was performed using electrospray ionization (ESI) and time of-flight (TOF) analyzer, in positiveion or negative-ion detection mode.

**1.2 Design and synthesis of compounds:** the synthetic routes of Bu-NISe and Gly-NISe were outlined in Scheme S1.

**1.2.1 Detailed synthetic procedure of R1:** R1 was synthesized according to a previously reported procedure.[1]

**1.2.2 Detailed synthetic procedure of Bu-NISe:** The diphenyl diselenide (0.78) was dissolved in absolute ethanol (20 ml) and the solution was cooled to 0℃ with an ice bath. NaBH4 (0.21 g) was then added to the solutions in batches under $N_2$ atmosphere. After the reaction mixture turned to be colorless, CuI (0.59 g) and R1 (0.83 g) were added. The reaction mixture was refluxed for another 30 min, cooled to room temperature, and then filtered. The filtrate was collected, evaporated and purified by a column chromatography on silica gel (petroleum ether/ ethyl acetate, 250/1) to afford Bu-NI-Se as a yellow solid. Yield: 45%. $^{1}H$ NMR (400 MHz, DMSO-d6) δ (ppm) 8.66 (d, 1H), 8.57 (d, 1H), 8.36 (d, 1H), 7.85 – 7.77 (m, 1H), 7.60 (dd, 3H), 7.43 (t, 3H), 4.24 – 4.12 (m, 2H), 1.72 (q, 2H), 0.99 (t, 3H).$^{13}C$ NMR (100 MHz, DMSO-d6): δ (ppm) 163.47, 163.44, 141.01, 135.00, 132.40, 131.65, 130.90, 130.72, 130.62, 129.48, 128.31, 128.23, 128.13, 123.27, 121.56, 39.87, 30.07, 20.26, 14.17. $^{77}Se$ NMR (DMSO-d6) δ (ppm) 387.56. $C_{22}H_{20}NO_2Se^{+}$, calcd. 410.0659, found 410.0657. $C_{44}H_{38}N_2O_4Se_2Na^{+}$, calcd. 841.1060, found 841.1070.

**1.2.3 Detailed synthetic procedure of R2:** The synthesis of R2 used a procedure similar to that of Bu-NISe. Diphenyl diselenide was first reduced by $NaBH_4$ and then reacted with 4-bromo-1, 8-naphthalic anhydride in presence of CuI. Yield: 40%. $^1$H NMR (400 MHz, $CDCl_3$) δ (ppm), 8.66 (d, 1 H), 8.61 (d, 1 H), 8.31 (d, 1 H), 7.85 (t, 1 H), 7.66 (d, 2 H), 7.43-7.50 (m, 4 H).

**1.2.4 Detailed synthetic procedure of Gly-NISe:** A mixture of glycine (75 mg), isopropanol (10 ml) and triethylamine (135 μl) was stirred for 10 min at room temperature. R2 (176 mg) was added and the mixture was refluxed for 2 h. The reaction mixture was cooled to room temperature, poured into 20 ml of water and acidified with 1M HCl to PH 4-5. After filtration, the cake was collected and purified by a column chromatography on silica gel (petroleum ether/ dichloromethane, 10/1, and 0.5% acetic acid) to afford Gly-NISe as a yellow solid. Yield: 62%. $^1$H NMR, (400 MHz, DMSO-d6), δ (ppm), 8.63 (d, 1 H), 8.58 (d, 1 H), 8.33 (d, 1 H), 7.96 (t, 1 H), 7.60-7.68 (m, 3 H), 7.40-7.50 (m, 3 H), 4.72 (s, 2 H). $^{13}$C NMR (100 MHz, DMSO-d6): δ (ppm) 169.70, 163.19, 163.17, 142.10, 135.19, 132.89, 132.09, 131.31, 130.88, 130.77, 130.44, 129.59, 128.46, 128.22, 127.90, 122.67, 120.82, 41.63. $^{77}$Se NMR, (DMSO-d6), δ (ppm), 390.62. $C_{20}H_{12}NO_4Se^-$, calcd. 409.9932, found 410.0001.

**2. Spectroscopic measurements.** The steady-state absorption spectra were recorded using a PerkinElmer Lambda 35 spectrophotometer, and the steady-state emission spectra were collected using a continuous (150 watts) FS5 fluorescence spectrometer equipped with a dinburg instrument. When testing the phosphorescence, nitrogen is used to bubble out the oxygen in the solution, and the low temperature phosphorescence test is realized in the liquid $N_2$ condition. The photoluminescence quantum yield of the solution was determined by integrating sphere spectrometer (FLS 1000). In order to ensure the accuracy of the test results, pure water was used as the standard sample to calibrate the instrument and measurement method. Time resolved fluorescence attenuation data were collected by time corrected single photon counting (TCSPC).

Nanosecond transient spectral emission was carried out with a self-built pump-

detection device, and the response time of the instrument was 100 ns. The laser energy used in the experimental test is less than 1 mJ/pulse, and the laser pulse wavelength used is 355 nm. All samples tested were bubbled with nitrogen for 45 min to remove oxygen from the solution.

The femtosecond transient spectral absorption measurements were carried out by using a femtosecond pump device built by us. The laser pulse of 80 fs and pulse wavelength of 800 nm were used in the measurements, and the femtosecond oscillator was generated by a regenerative amplifier. The measurement uses thin $CaF_2$ plates to generate supercontinuum spectrum. The mutual polarization between the pump beam and the probe beam was set to a magic angle of 54.7° by placing a Berek compensator in the pump beam. The delay between the pump and the probe pulse was controlled by an electric delay. The dynamic energy of the different scans remained the same and there was no sign of change during the measurements. The FSTA spectra were measured through using a quartz colorimetric tube with path length of 1 mm at room temperature.

**3. Theoretical calculations.** The ground ($S_0$) and first singlet excited states ($S_1$) geometries of Bu-NISe and Gly-NISe in different solvents were determined at Cam-b3lyp/6-311G (d, p) level using DFT and TD-DFT methods. The solvent effects were included by the integral equation formalism (IEF) version of the polarizable continuum model (PCM). The frequency calculations at the same level of theory were then performed to confirm that each optimized structure was the real minimum. All the DFT and TDDFT calculations were carried out by using the Gaussian 09 program.[2] The spin-orbit coupling matrix elements of the molecule were computed based on the optimized $S_0$ geometries by employing the PySoc program.[3]

**4. Cell culture.** Cell lines were cultured in the Dulbecco's modified Eagle's medium (DMEM) containing 10% fetal bovine serum (FBS), and 1% penicillin-streptomycin under 100% humidity, at 37 °C with 5% $CO_2$ incubator.

## Part Ⅱ: Schemes, Equations, Tables and Figures

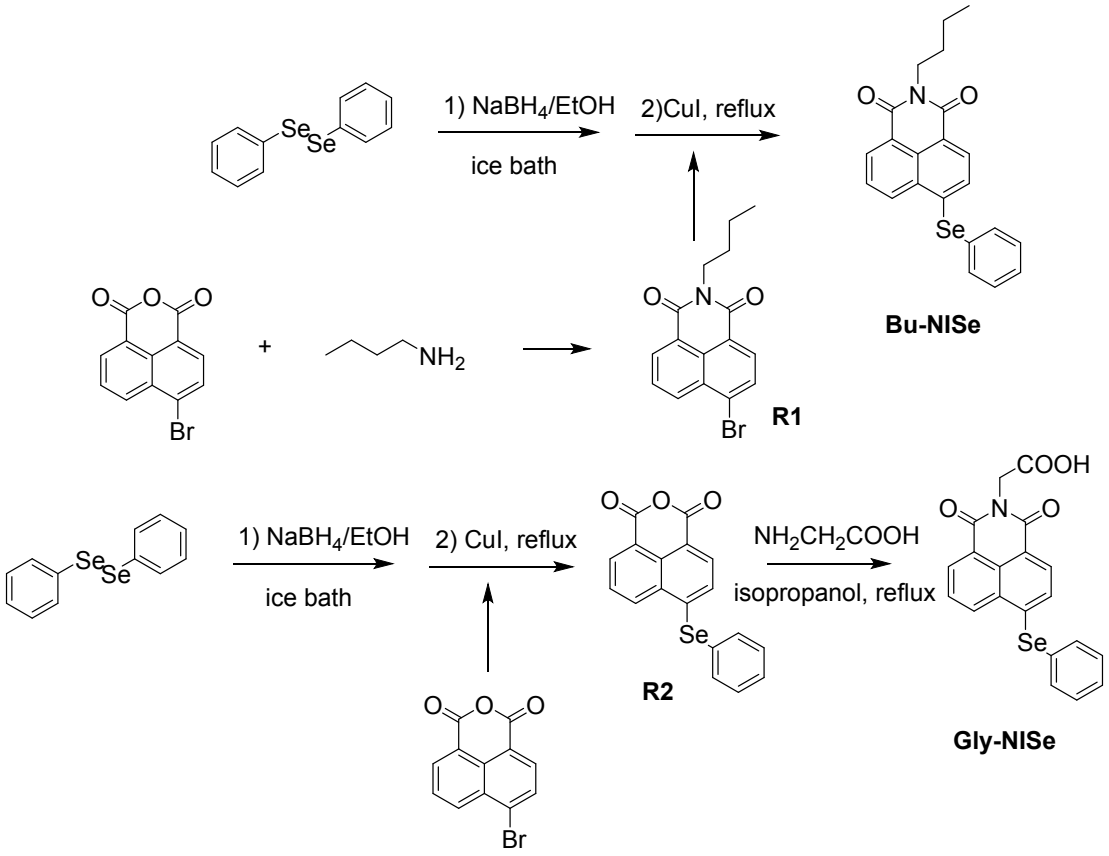


**Scheme S1.** Outlines of synthetic routes of Bu-NISe and Gly-NI-Se

$$\Phi_{\mathrm{p}} = \Phi_{isc} k_p \tau_p$$ **Equation (1)**

$$\Phi_{isc} = k_{isc} / \left( k_f + k_{ic} + k_{isc} \right)$$ **Equation (2)**

**Equations (1) and (2).** The quantitative relationship between the ISC rate and phosphorescence efficiency. Here $\Phi_p$ is the phosphorescence quantum yield, $\Phi_{isc}$ is the quantum yield of intersystem crossing, $k_p$ is the radiative decay rate of $T_1$-$S_0$. $\tau_p$ represent the phosphorescence emission lifetime. $k_f$ and $k_{ic}$ represent the radiative and IC decay rates of $S_1$-$S_0$ respectively. $k_{isc}$ is the ISC rate.

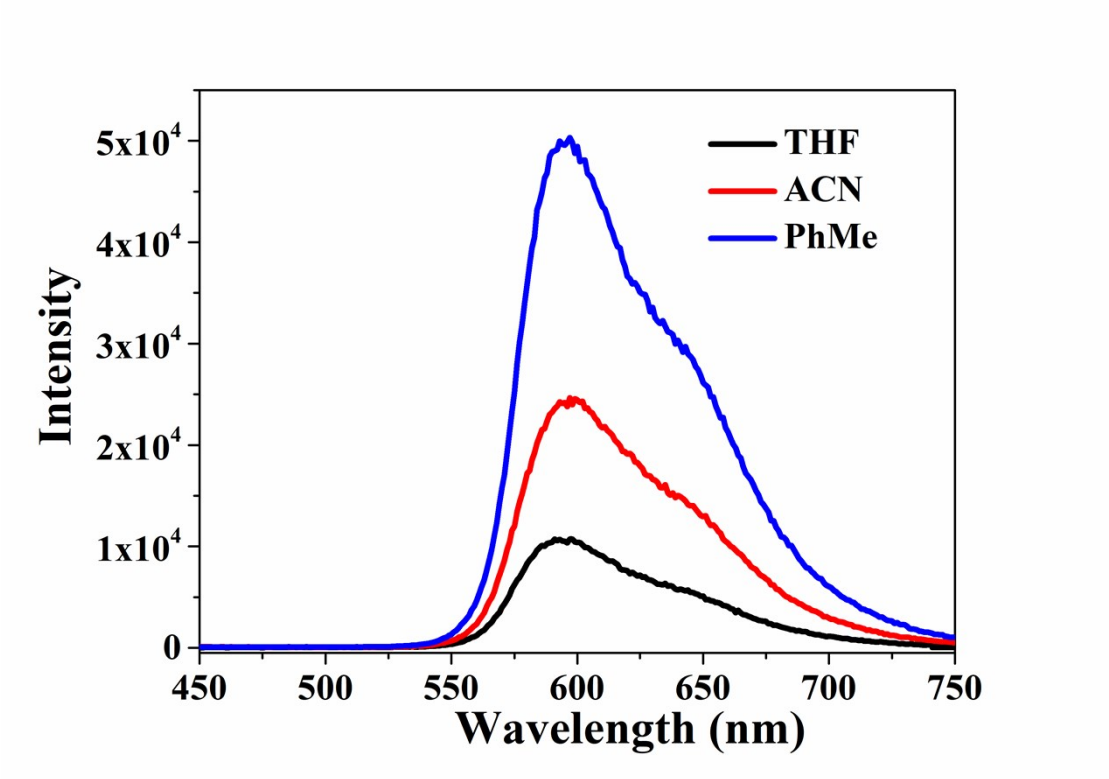


**Figure S1.** Phosphorescence spectra for Bu-NISe molecule in different solvents. (blue line: PhMe, black line: THF, red line: ACN).

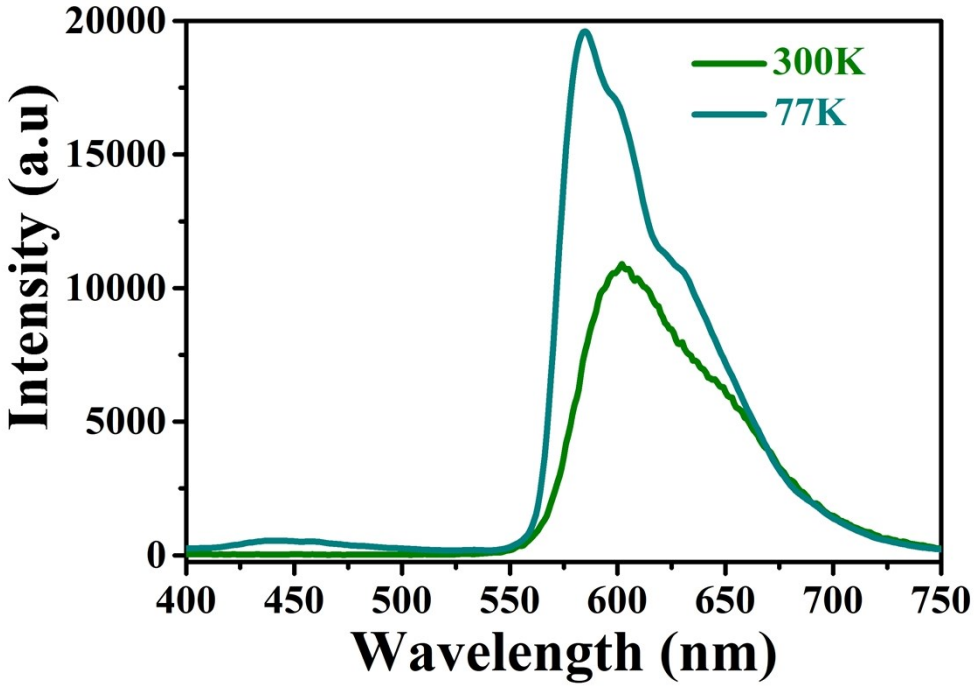


**Figure S2.** Phosphorescence spectrum of Bu-NISe at 77 K and 300 K under ambient condition (25 μM). Excitation:λ=393 nm.

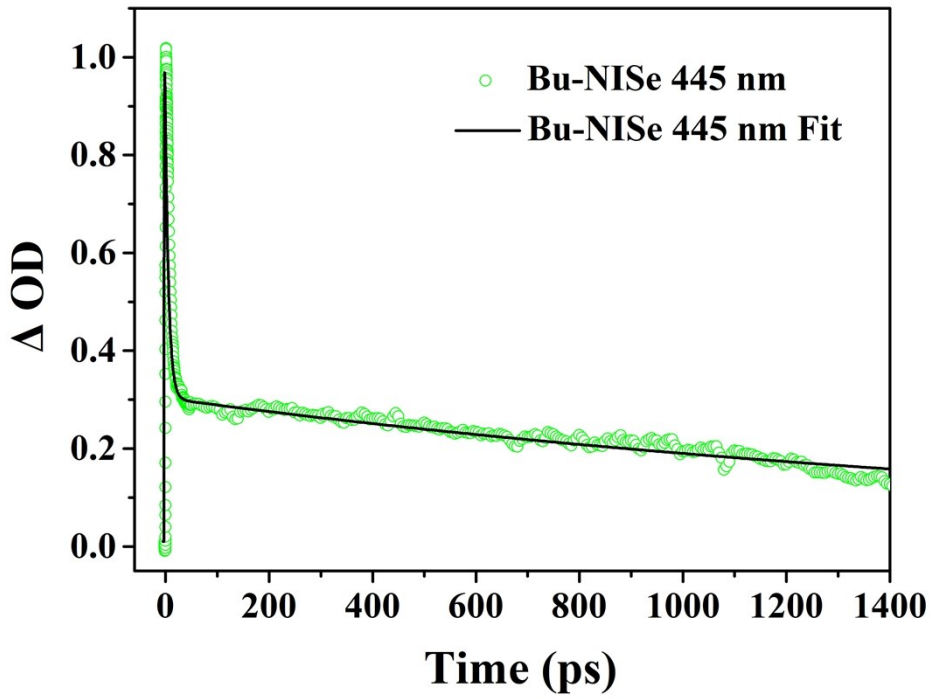


**Figure S3.** Transient PL decay of Bu-NISe at 445 nm.

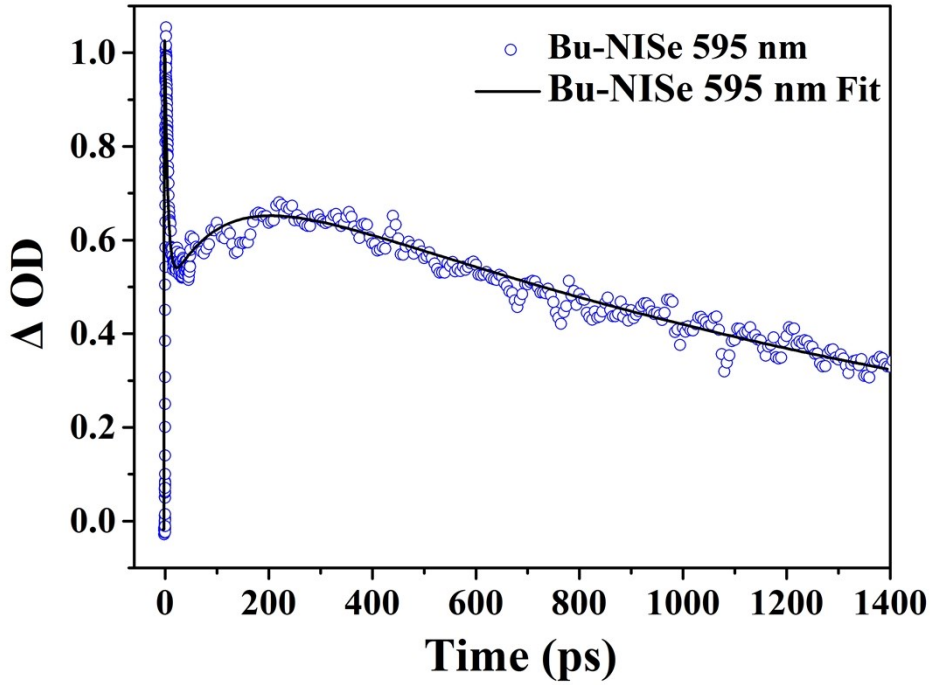


**Figure S4.** Transient PL decay of Bu-NISe at 595 nm.

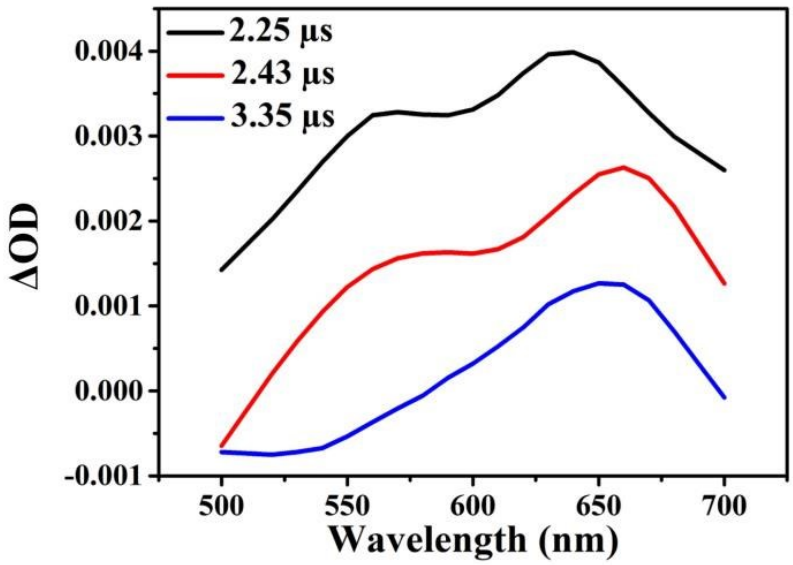


**Figure S5.** The nanosecond transient absorption spectra of Bu-NISe (25 μM) in toluene with $N_2$ condition. Excitation:λ=355 nm.

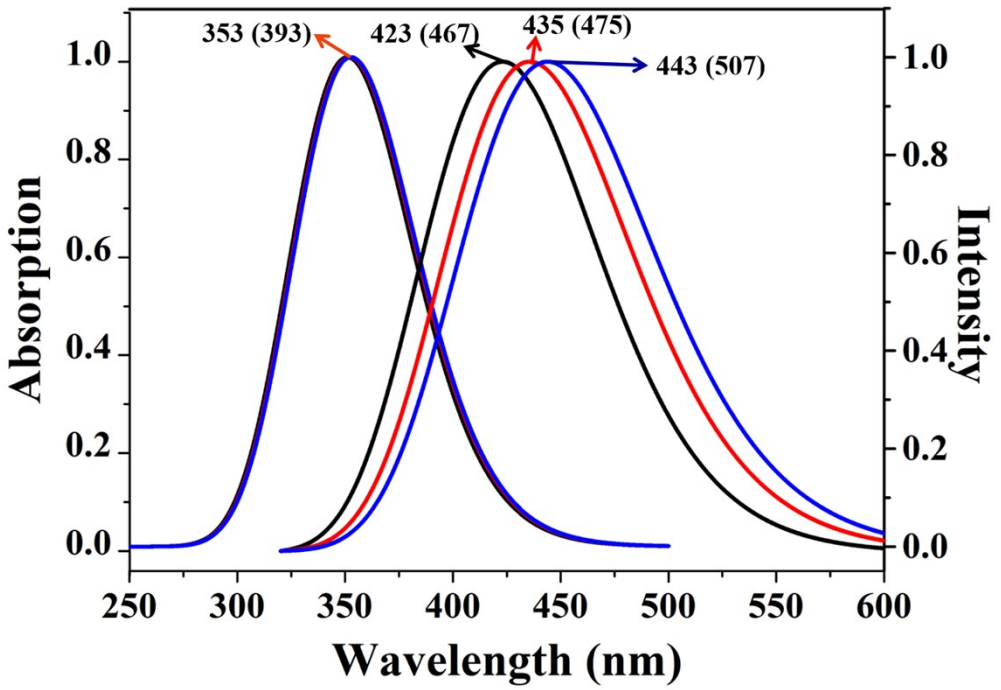


**Figure S6.** The TD-CAM-B3LYP/6-311G(d,p) calculated absorption spectra and Fluorescence spectra for Bu-NISe molecule in different solvents (black line: PhMe, red line: THF, blue line: ACN). The experimental values are provided in parentheses.

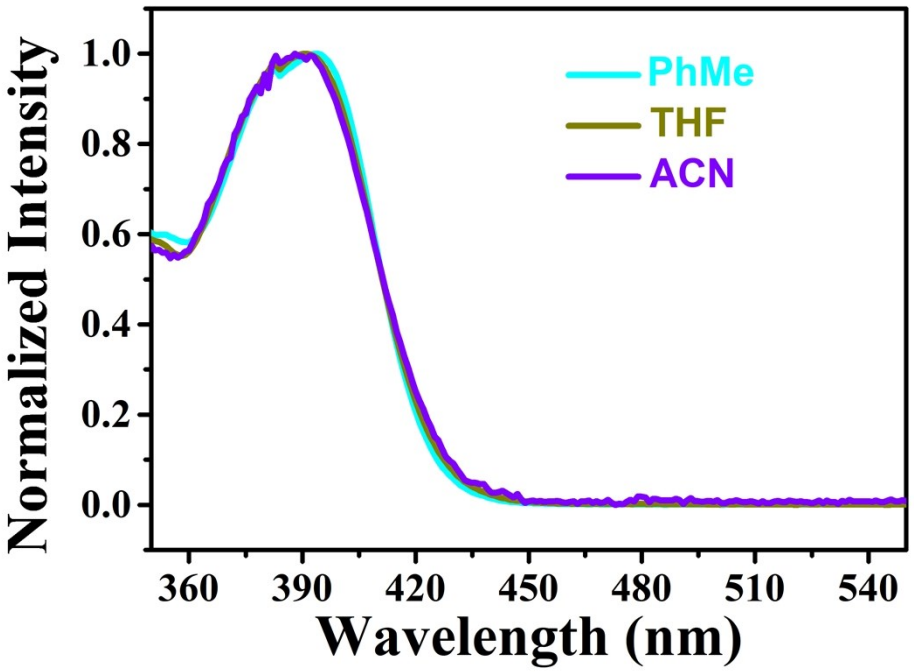


**Figure S7.** Absorption spectra of Bu-NISe (25 μM) in different solvents with ambient condition. Symbols: PhMe, toluene; THF, tetrahrdrofuran; ACN, acetonitrile.

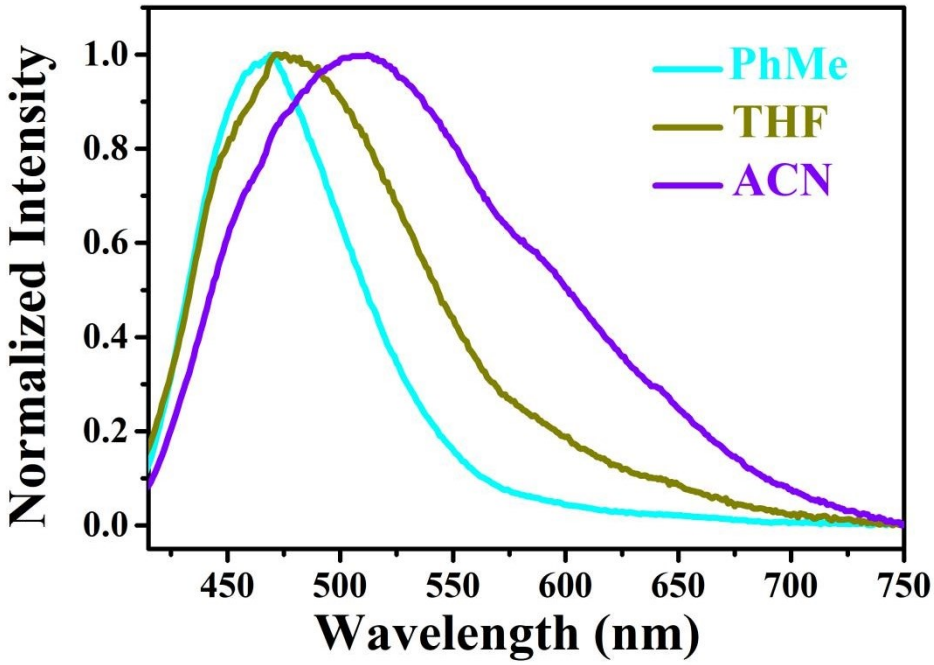


**Figure S8.** Fluorescence spectra of Bu-NISe (25 μM) in different solvents with ambient condition. Excitation: λ=393 nm. Symbols: PhMe, toluene; THF, tetrahrdrofuran; ACN, acetonitrile.

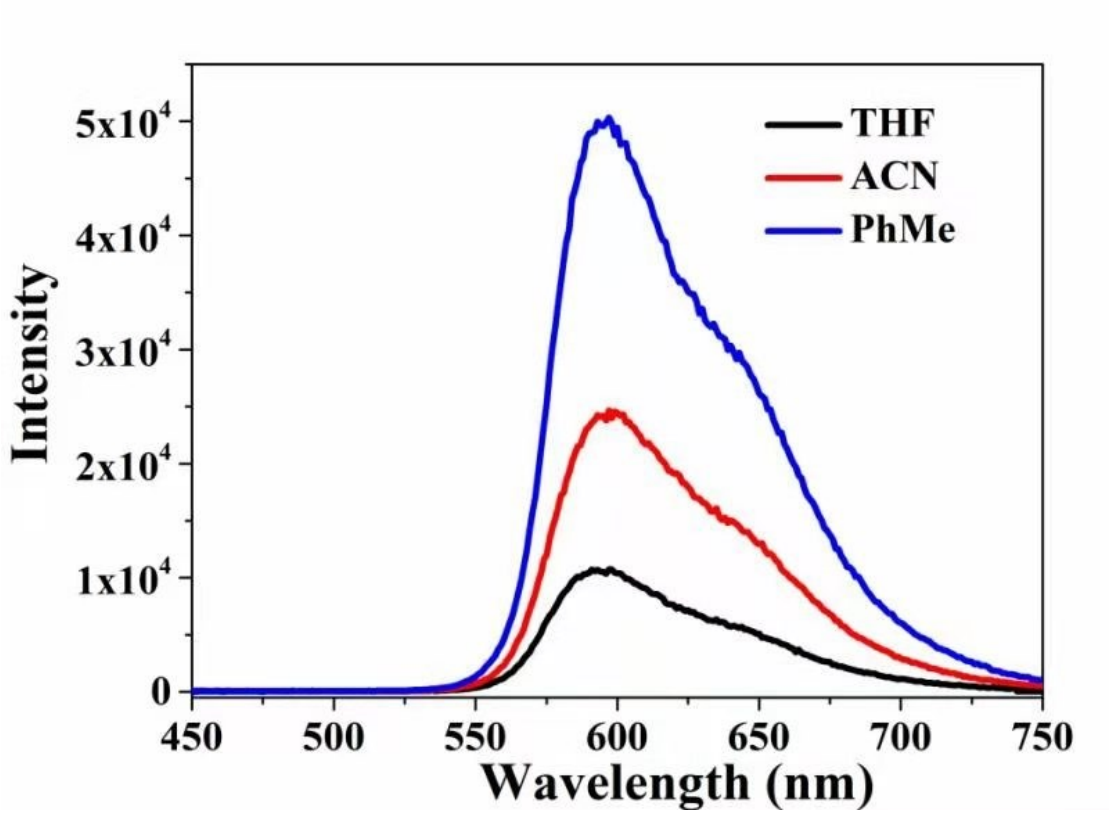


**Figure S9.** Phosphorescence spectra of Bu-NISe (25 μM) in different solvents with $N_2$ condition. Excitation: λ=393 nm. Symbols: PhMe, toluene; THF, tetrahrdrofuran; ACN, acetonitrile.

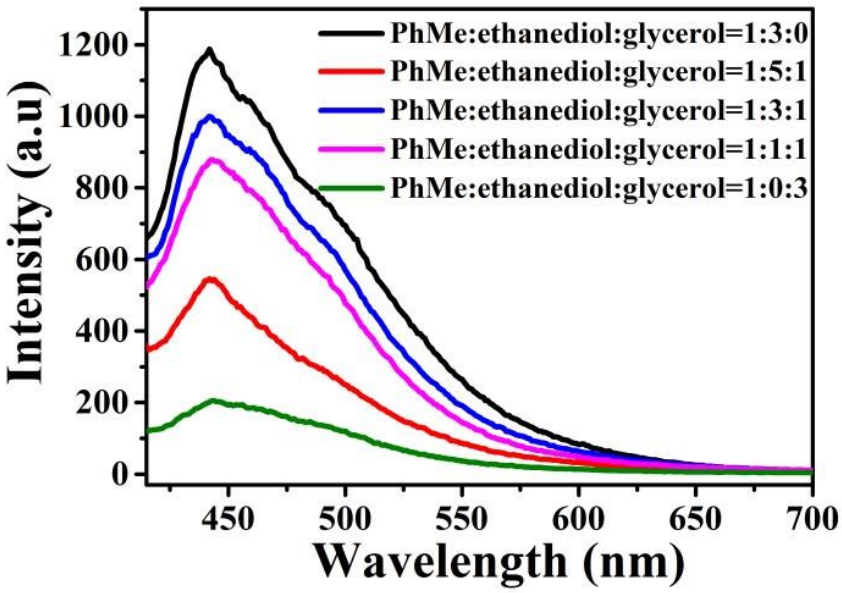


**Figure S10.** The fluorescence response of Bu-NISe to viscosity with ambient condition. The ambient viscosity was adjusted by the ratios of toluene (PhMe), ethanediol and glycerol solvents.

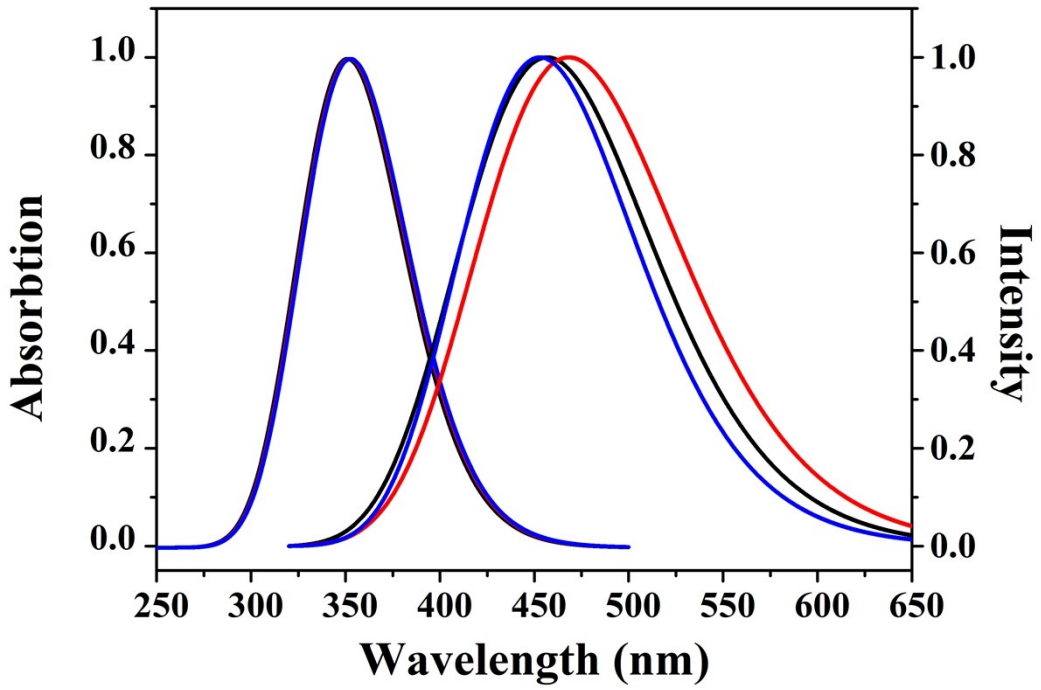


**Figure S11.** Absorption spectra and Fluorescence spectra for Gly-NISe molecule in different solvents (black line: PhMe, red line: THF, blue line: ACN), calculated Cam-B3LYP/6-311G (d,p) level using DFT and TDDFT method.

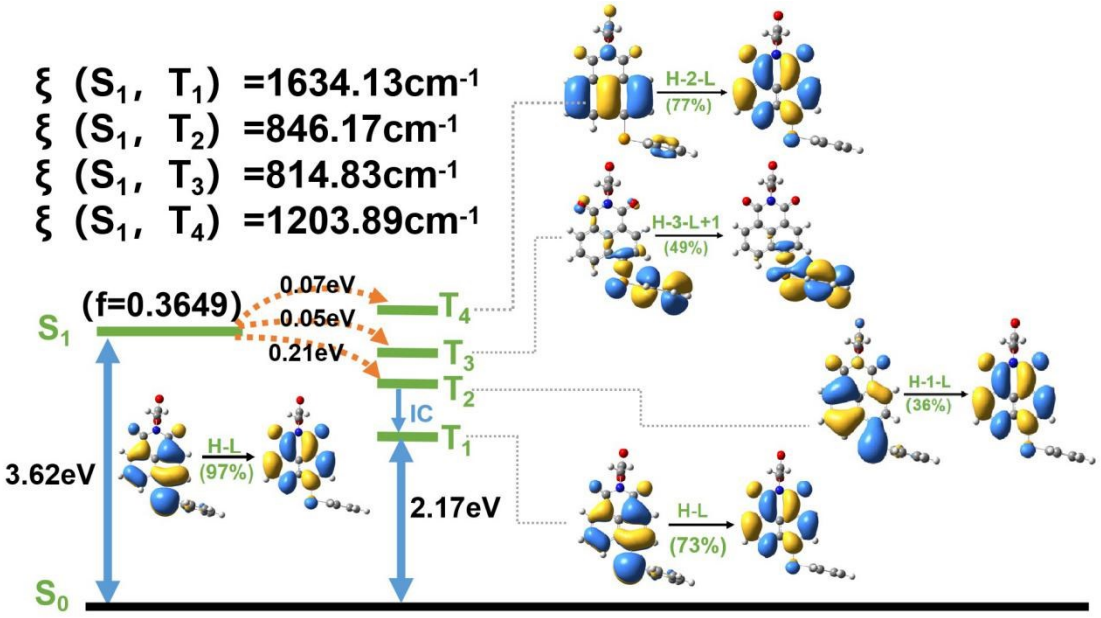


**Figure S12.** Schematic diagrams showing the TD-DFT calculated results of Gly-NISe. Included are energy levels, isosurface and main molecular orbital configurations percentage of Gly-NISe at singlet ($S_1$) and triplet states ($T_n$) based on the optimized ground state geometries. The orange dashed arrows represent the ISC processes probably occurring from the $S_1$ state to $T_n$ states. HOMO and LUMO refer to highest occupied molecular orbital and lowest unoccupied molecular orbital, respectively. The values in parentheses indicate the orbital contribution at different electron excitations.

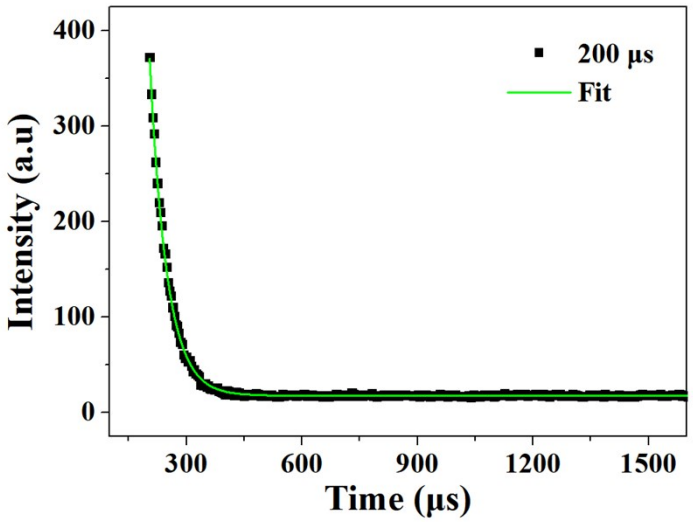


**Figure S13.** Decay curve of Gly-NISe phosphorescence intensity over time in PBS with deoxygenated.

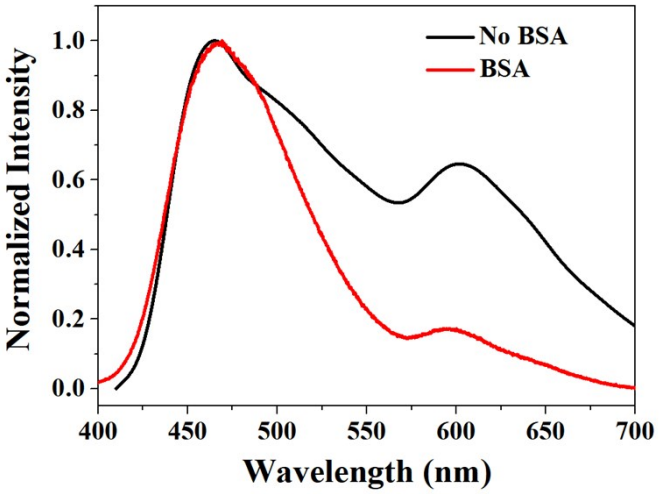


**Figure S14**. Steady-state emission spectra of probe GlyNISe in DMSO (black) and a suspension of GlyNISe in DMSO/$H_2O$ (red) and bovine serum albumin (BSA) aqueous solution under $N_2$ condition. (λex=390 nm). (The binding of the probe to cellular proteins can occur, but non-specific phosphorescence enhancement would not be caused by this binding).

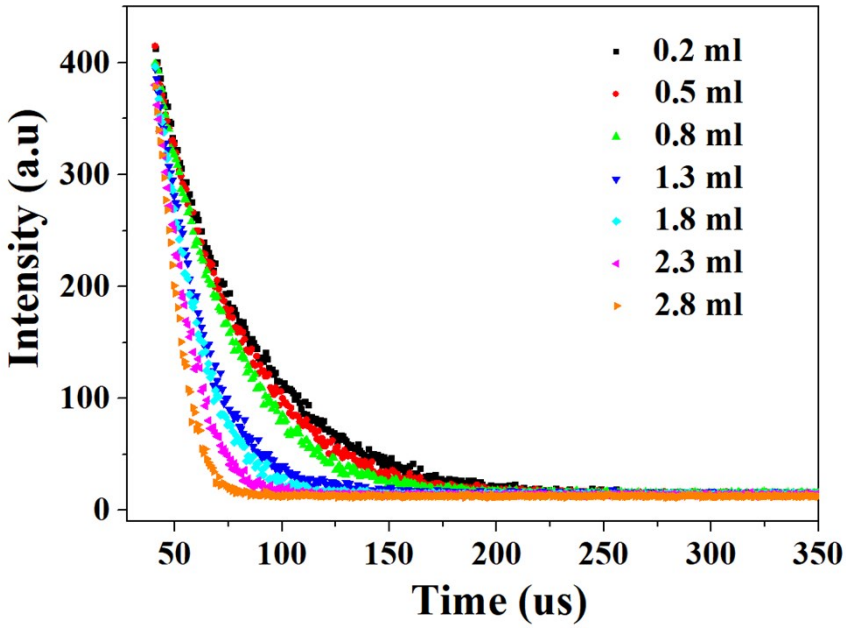


**Figure S15.** Oxygen-dependent transient PL spectra of Gly-NISe (0.2 mg $ml^{-1}$) in PBS solution, λex = 393 nm.

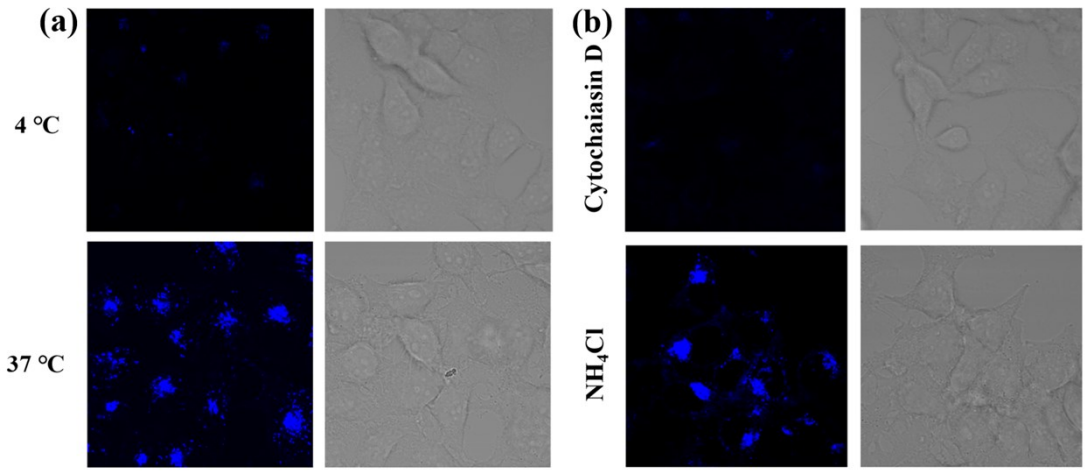


**Figure 16.** (a) Fluorescent and bright field images of HeLa cells stained with GlyNISe ($1 \times 10^{-6}$ M, 10 min), at different temperature 4 and 37 °C. Scale bar = 10 μm. (b)The fluorescent and bright field images of HeLa cells pretreated with endocytic inhibitors $NH_4Cl$ ($50 \times 10^{-3}$ M), Cytochalasin D ($5 \times 10^{-6}$ M), respectively and then incubated with GlyNISe ($1 \times 10^{-6}$ M) 37 °C for 30 min. (These results suggested an endocytotic mechanism for Gly-NISe internalization by cells .)

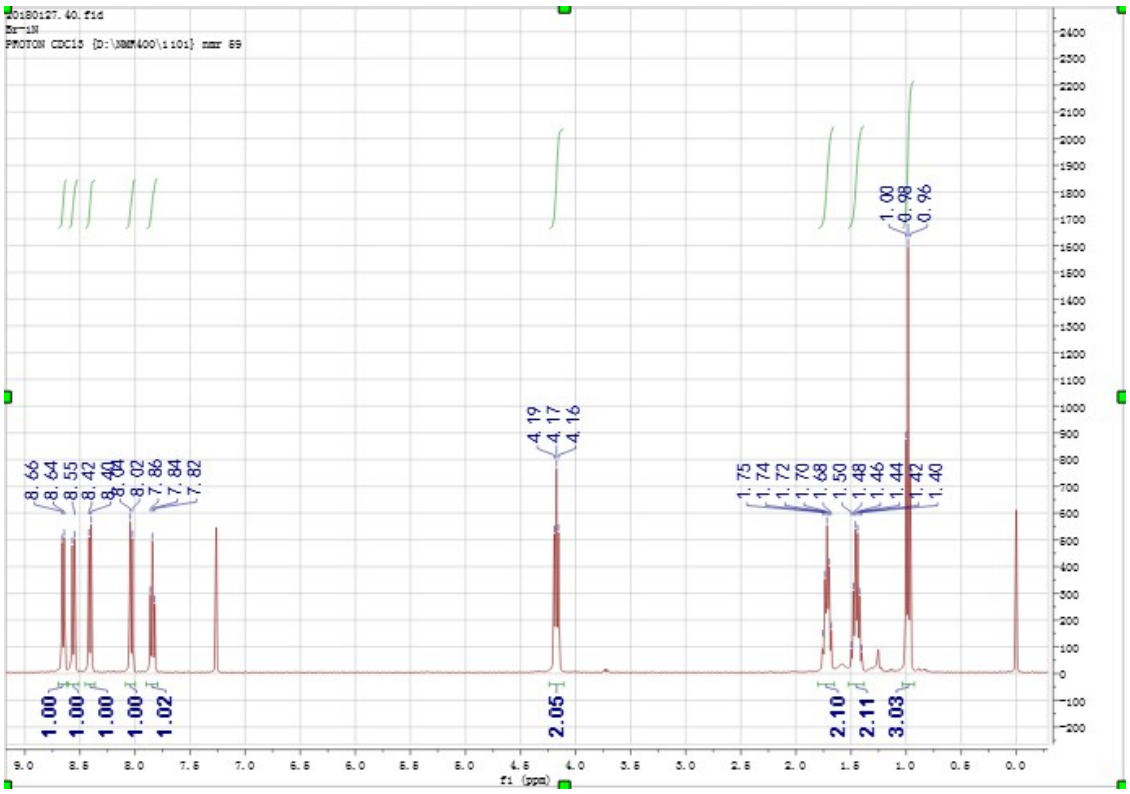


**Figure S17.** $^{1}H$ NMR spectrum of $R_1$ in $CDCl_3$

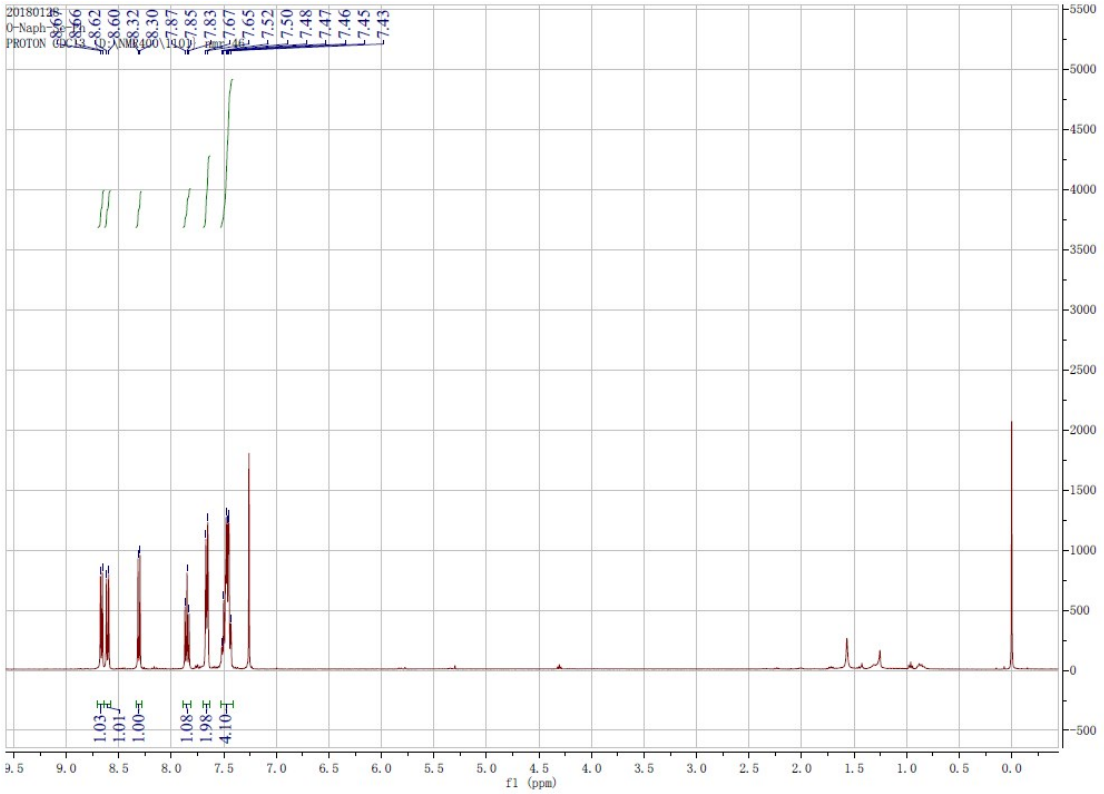


**Figure S18.** $^{1}H$ NMR spectrum of $R_2$ in $CDCl_3$

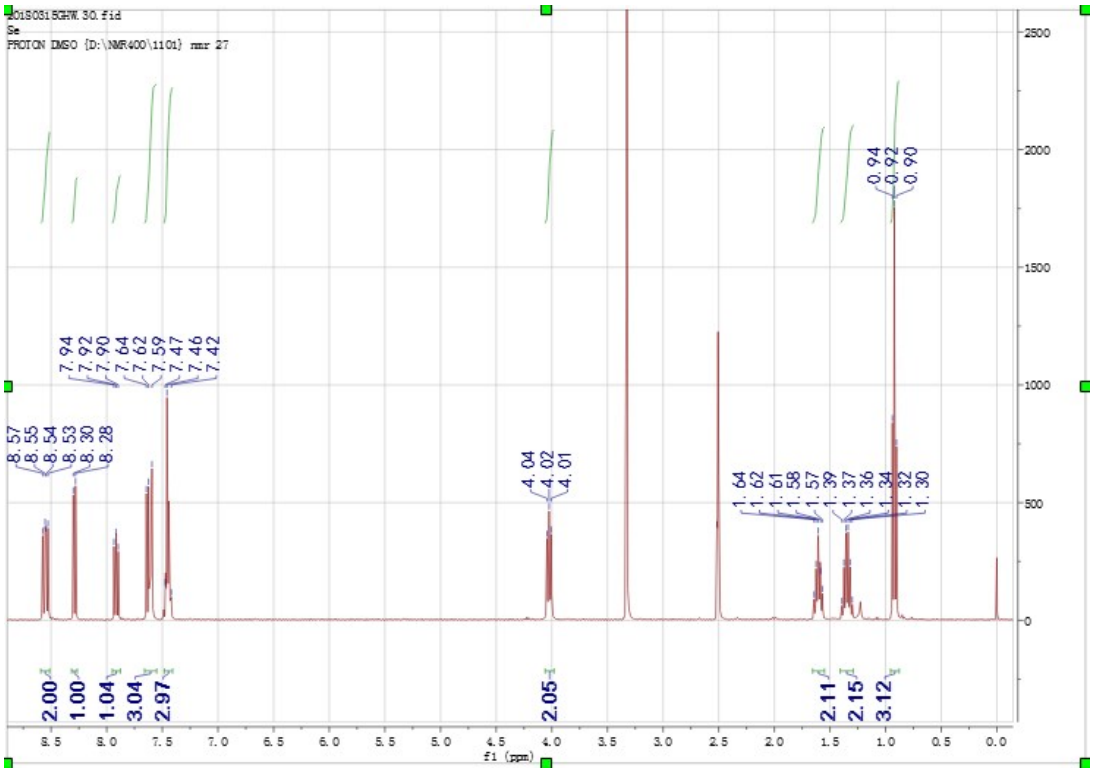


**Figure S19.** $^{1}H$ NMR spectrum of Bu-NISe in DMSO-$d_6$

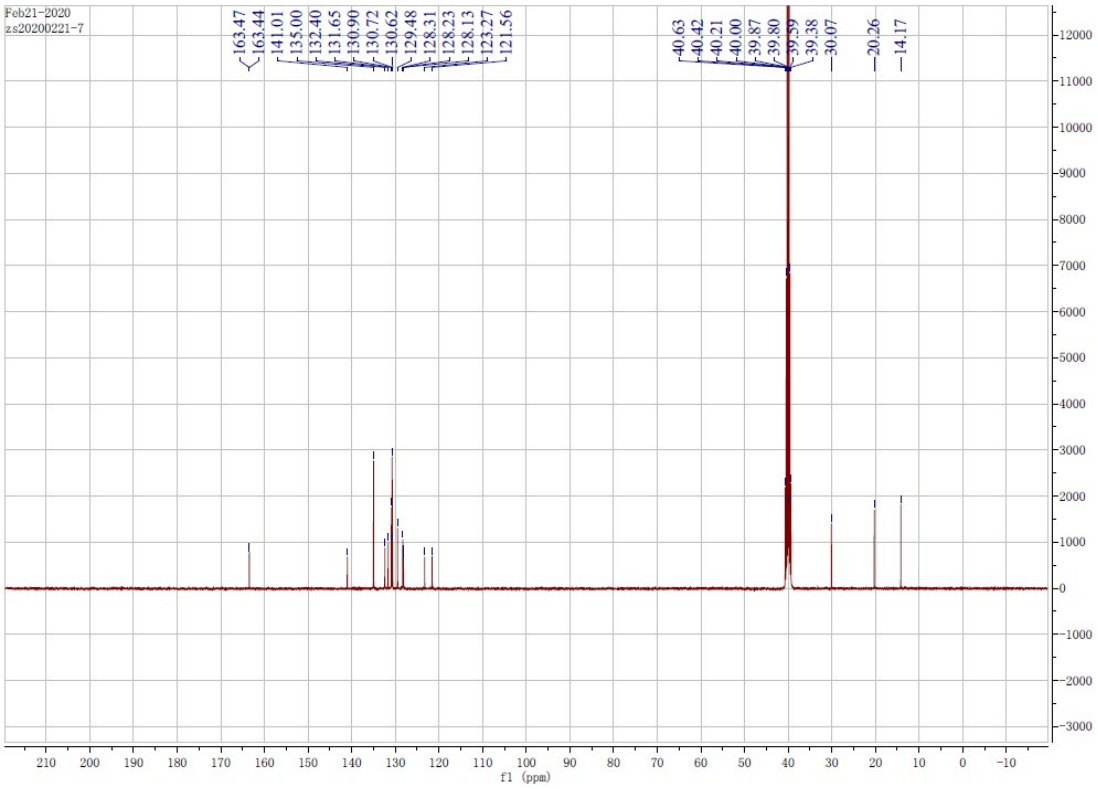


**Figure S20.** $^{13}C$ NMR spectrum of Bu-NISe in DMSO-$d_6$

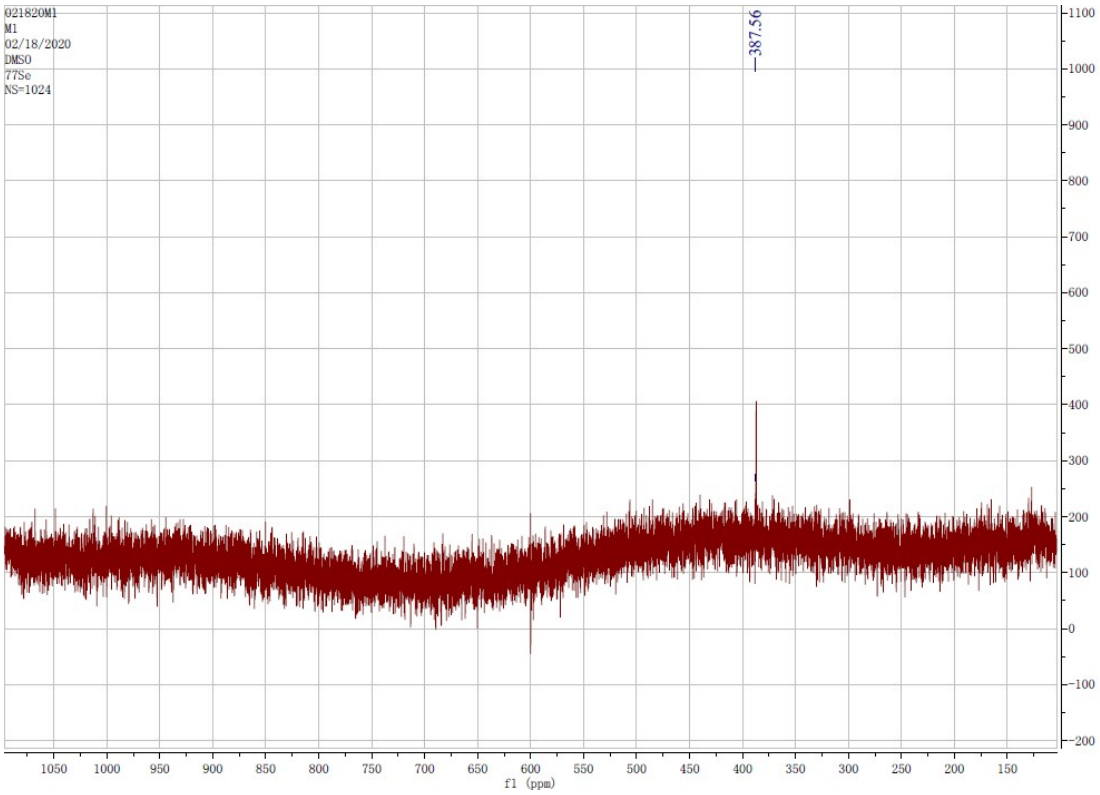


**Figure S21.** $^{77}$Se NMR spectrum of Bu-NISe in DMSO-$d_6$

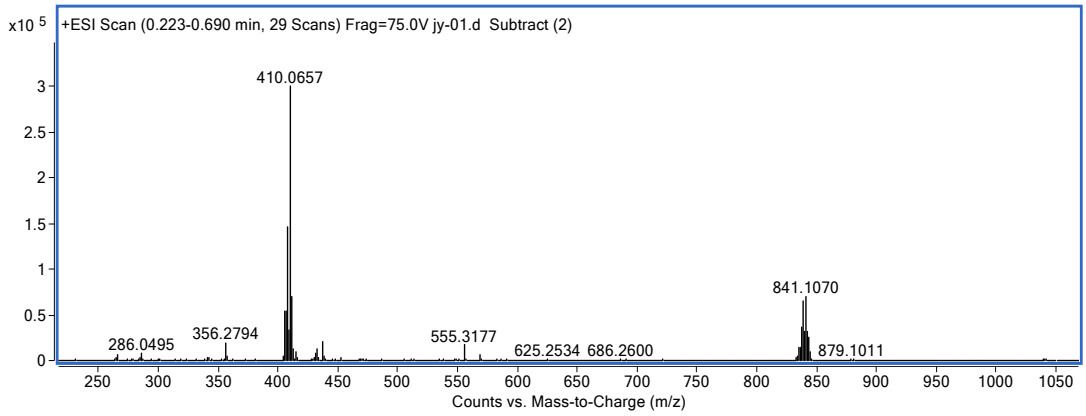


**Figure S22.** HRMS spectrum of Bu-NISe ($ESI^+$)

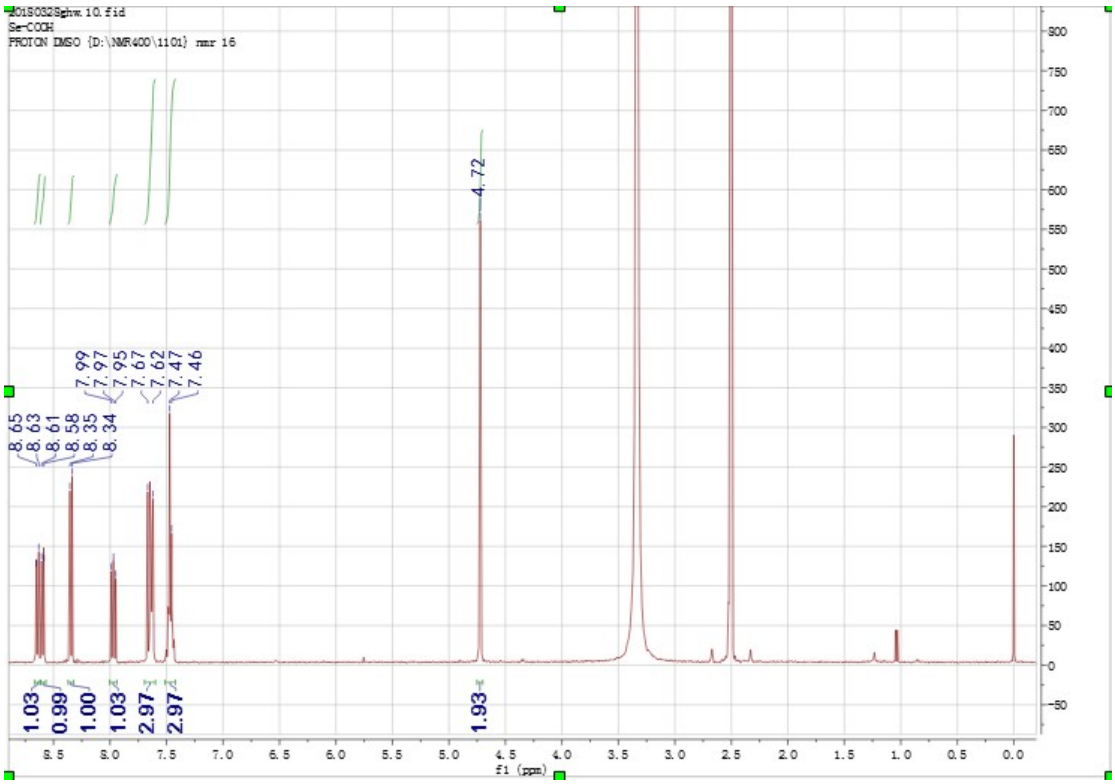


**Figure S23.** $^{1}$H NMR spectrum of Gly-NISe in DMSO-$d_6$

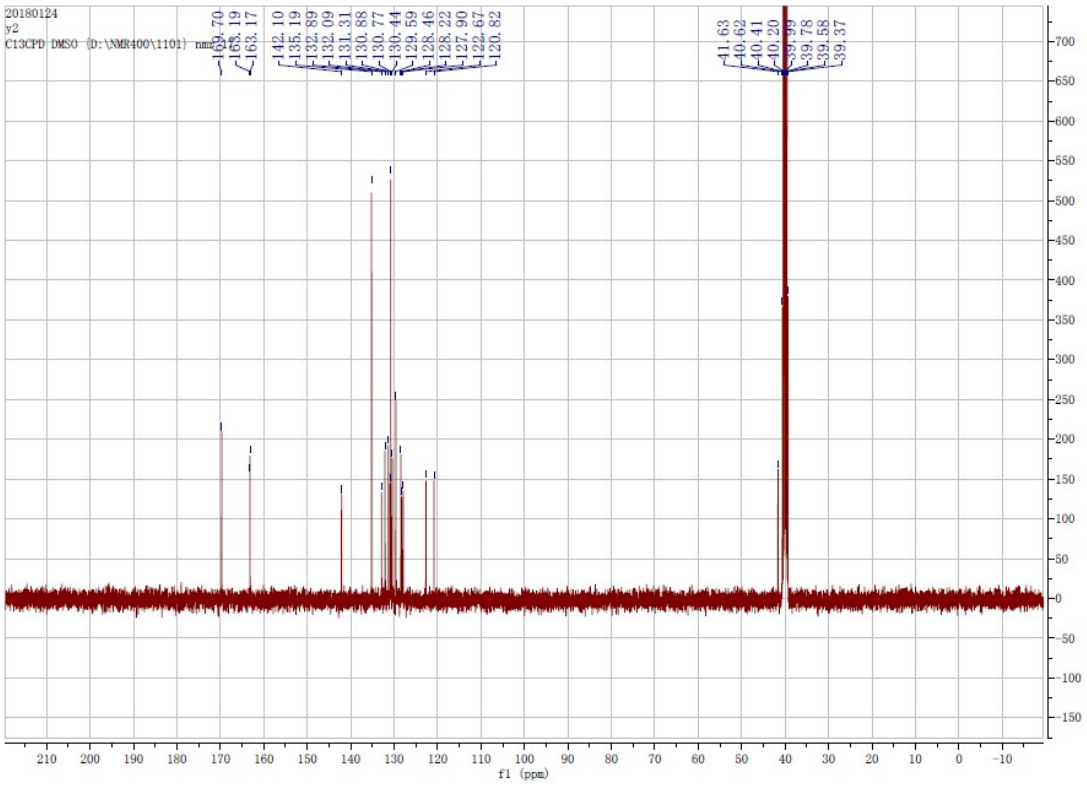


**Figure S24.** $^{13}C$ NMR spectrum of Gly-NISe in DMSO-$d_6$

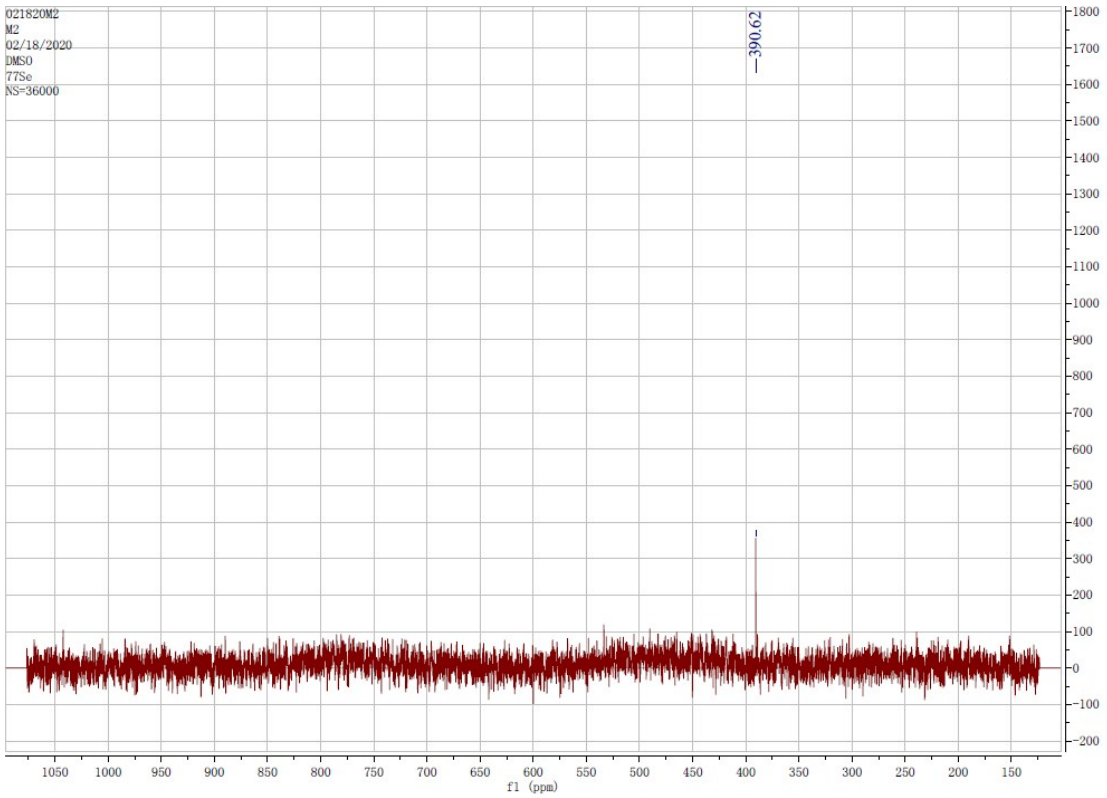


**Figure S25.** $^{77}$Se NMR spectrum of Gly-NISe in DMSO-$d_6$

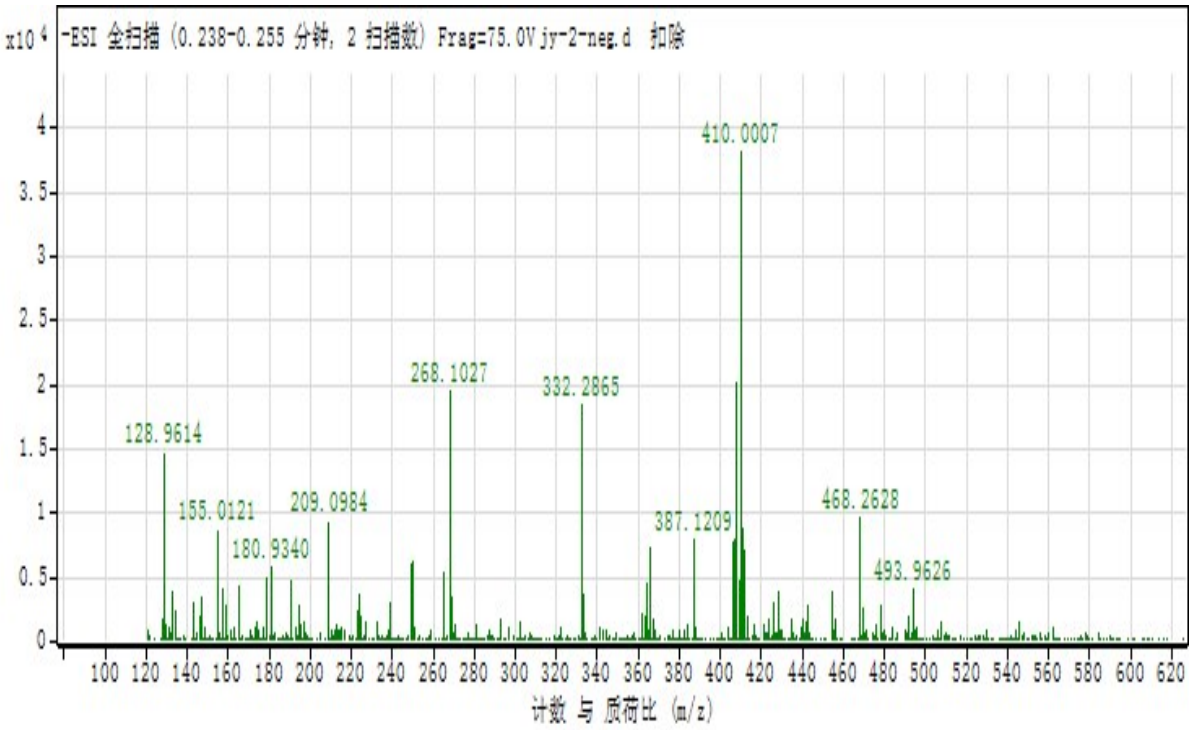


**Figure S26.** HRMS spectrum of Gly-NISe ($ESI^-$)

**Table S1**. The phosphorescence quantum yields of Gly-NISe and some metal-complexes reported in literatures. These metal-complexes were used for biological imaging or as standard sample for determining the quantum yields of phosphorescent molecules. The quantum yields of the metal-complexes are given as luminecesnce (including phosphorescence and fluorescence) quantum yields.

| Compounds | Φp | references |
|---|---|---|
| Gly-NISe | 0.04 | this work |
| 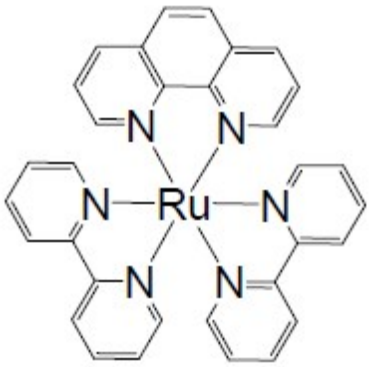 | 0.06 | Glazer et.al, J. Am. Chem. Soc.,2007,129:8544-8551 |
| 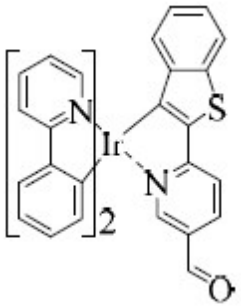 | 0.07 | Zheng et. al, Nat. Biomed. Eng. |
| 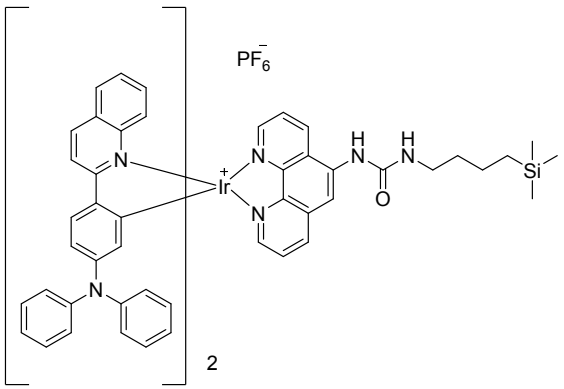 | 0.05 | Lv et.al, Adv. Sci. 2015, 2, 1500107 |

| | | | |
|---|---|---|---|
| 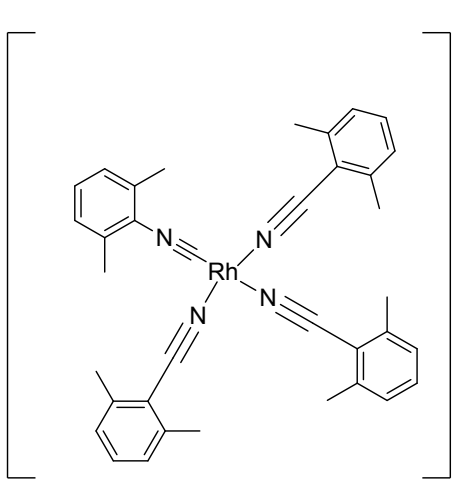 | $SO_4^{2-}$ | 0.02 | Wang et.al, J. Am. Chem. Soc. 2020, 142, 2709−2714 |

**Table S2** The excited state dynamic process of Bu-NISe at different wavelength based on decays of fs-TA spectra.

| | A1 | $\tau_1$ (ps) | A2 | $\tau_2$ (ps) | A3 | $\tau_3$ (ps) |
|---|---|---|---|---|---|---|
| 445 nm | -0.013 | 0.5 | 0.018 | 6.5 | 0.006 | 2054 |
| 510 nm | -0.008 | 3.0 | 0.01 | 0.4 | 0.0045 | 2084 |
| 595 nm | -0.006 | 0.4 | 0.007 | 6.0 | 0.008 | 1605 |
| 645 nm | 0.005 | 1.8 | -0.003 | 56 | 0.009 | 2529 |

**Table S3.** The fluorescence, phosphorescence intensity quantitative and the ratio of luminescence images for BEL-7402 cells stained with Gly-NISe based on laser scanning confocal microscopy (LSCM). Excitation wavelength: 405 nm.

| Condition | Fluorescence (a.u.) | Phosphorescence (a.u.) | Ratio |
|---|---|---|---|
| 1% $O_2$ | 161.09 | 162.55 | 1.01 |
| 5% $O_2$ | 156.50 | 145.01 | 0.93 |
| 10% $O_2$ | 155.76 | 118.54 | 0.76 |
| Air | 159.27 | 67.34 | 0.42 |

**Table S4.** Geometry Data for Bu-NISe ($S_0$ optimization: unit Å)

| Atom | x | y | z |
|---|---|---|---|
| C | -1.33863900 | 0.70818700 | 1.37489100 |
| C | -0.56588200 | -0.27696700 | 0.72104400 |
| C | 0.84631300 | -0.27198800 | 0.85644400 |
| C | 1.43341400 | 0.72635700 | 1.66889400 |
| C | 0.66351700 | 1.67068300 | 2.29426300 |
| C | -0.73264100 | 1.66847900 | 2.14421100 |
| C | -1.20309600 | -1.27008800 | -0.05626900 |
| C | -0.46062200 | -2.23146800 | -0.68740800 |
| C | 0.94111400 | -2.22758700 | -0.57919100 |
| C | 1.59068000 | -1.27576500 | 0.16722800 |
| C | -2.81572200 | 0.71577500 | 1.24347700 |
| N | -3.39242900 | -0.30350000 | 0.48455200 |
| C | -2.67972000 | -1.28619700 | -0.19906700 |
| O | -3.25331300 | -2.11407400 | -0.87368900 |
| O | -3.50764000 | 1.55984000 | 1.77051200 |
| C | -4.85633000 | -0.31283500 | 0.35897600 |
| C | -5.34499700 | 0.51259400 | -0.82477200 |
| C | -6.86576900 | 0.49373000 | -0.94213800 |
| C | -7.37607700 | 1.31507100 | -2.12111200 |
| C | 4.04599300 | 0.21501100 | -0.55175600 |
| C | 5.21573100 | 0.82373900 | -0.10960000 |
| C | 5.68165700 | 1.96893000 | -0.74191400 |
| C | 4.97412200 | 2.51964000 | -1.80087900 |
| C | 3.80177600 | 1.91347200 | -2.23318500 |
| C | 3.34058600 | 0.75736800 | -1.61974900 |
| H | 2.50731900 | 0.73074900 | 1.79523400 |
| H | 1.13312900 | 2.42525800 | 2.91283800 |
| H | -1.35102500 | 2.41098900 | 2.63221600 |

| | | | |
|---|---|---|---|
| H | -0.96925600 | -2.98281500 | -1.27791200 |
| H | 1.51651600 | -2.98056900 | -1.10205500 |
| H | -5.15853500 | -1.35257500 | 0.24866000 |
| H | -5.25725700 | 0.08309600 | 1.29011400 |
| H | -4.99728200 | 1.54343300 | -0.70824400 |
| H | -4.89978400 | 0.11778300 | -1.74308500 |
| H | -7.20770700 | -0.54198100 | -1.04233900 |
| H | -7.30475500 | 0.87448100 | -0.01366100 |
| H | -8.46587900 | 1.28707500 | -2.18478400 |
| H | -6.97777800 | 0.93624000 | -3.06601600 |
| H | -7.07482000 | 2.36201500 | -2.03068200 |
| H | 5.76049900 | 0.41019500 | 0.73116100 |
| H | 6.59545700 | 2.43675900 | -0.39539700 |
| H | 5.33339200 | 3.41821800 | -2.28726800 |
| H | 3.24474500 | 2.33643000 | -3.06076500 |
| H | 2.43433000 | 0.28185700 | -1.97345500 |
| Se | 3.50590800 | -1.42279800 | 0.30984300 |

**Table S5.** Geometry Data for Gly-NISe ($S_0$ optimization: unit Å)

| Atom | x | y | z |
|---|---|---|---|
| C | 0.94944500 | -0.69861500 | -1.82509100 |
| C | -0.42114400 | -1.03236500 | -1.80037400 |
| C | -1.31211700 | -0.28161400 | -1.04701200 |
| C | -0.85082800 | 0.83300500 | -0.29600200 |
| C | 0.53955400 | 1.17166300 | -0.31261700 |
| C | 1.42233100 | 0.37538700 | -1.09628700 |
| C | -2.74065300 | -0.64362800 | -1.03084400 |
| C | -1.75474400 | 1.61378800 | 0.47573700 |
| C | -3.19108400 | 1.27754900 | 0.50209700 |

| | | | |
|---|---|---|---|
| C | -1.29151000 | 2.70007500 | 1.20550000 |
| C | 0.07995800 | 3.03740300 | 1.18892300 |
| C | 0.97582400 | 2.28908300 | 0.44851900 |
| H | 2.03295800 | 2.51966900 | 0.40656100 |
| H | 0.42785700 | 3.89004000 | 1.76163100 |
| H | 1.63623300 | -1.28320800 | -2.42540900 |
| H | -0.80096000 | -1.87537700 | -2.36625200 |
| N | -3.59769800 | 0.17173900 | -0.27112000 |
| O | -3.20779200 | -1.62093800 | -1.65338000 |
| O | -4.02817900 | 1.93195300 | 1.15927200 |
| C | -5.01055600 | -0.20824200 | -0.23982900 |
| H | -5.55271500 | 0.61925800 | 0.22571500 |
| H | -5.37886500 | -0.36401700 | -1.25465000 |
| C | -5.29800700 | -1.47131600 | 0.54191700 |
| O | -6.33806600 | -2.12117700 | 0.43621700 |
| O | -4.30049700 | -1.79283300 | 1.43184800 |
| H | -4.53410300 | -2.61181800 | 1.92015400 |
| Se | 3.32230800 | 0.80514000 | -1.15908700 |
| C | 3.88012700 | -0.45288600 | 0.21568000 |
| C | 3.85852600 | -0.09083300 | 1.56402600 |
| C | 4.31287800 | -1.72094500 | -0.17823300 |
| C | 4.27445400 | -1.01412900 | 2.53013700 |
| H | 3.52643500 | 0.89864000 | 1.85670500 |
| C | 4.73168700 | -2.64090000 | 0.78888000 |
| H | 4.33158000 | -1.97662000 | -1.23179300 |
| C | 4.70805500 | -2.28870100 | 2.14395600 |
| H | 4.26000600 | -0.74194700 | 3.58061600 |
| H | 5.07167600 | -3.62690000 | 0.48876500 |
| H | 5.03142600 | -3.00199900 | 2.89524800 |

| | | | |
|---|---|---|---|
| H | -2.00302500 | 3.27865200 | 1.78334400 |

**References:**

1. Ren, J.; Wu, Z.; Zhou, Y.; Li, Y.; Xu, Z. X. Colorimetric fluoride sensor based on 1,8-naphthalimide derivatives. *Dyes Pigment.* 2011, 91 (3), 442-445.

2. Frisch, M.J., Trucks, G.W., Schlegel, H.B., Scuseria, G.E., Robb, M.A., Cheeseman, J.R., Scalmani, G., Barone, V., Mennucci, B., Petersson, G.A., et al.Gaussian, Inc.: Wallingford, CT, USA. 2009.

3. Xing Gao, Shuming Bai, Daniele Fazzi, Thomas Niehaus,§ Mario Barbatti, and Walter Thiel Evaluation of Spin-Orbit Couplings with Linear-Response TimeDependent Density Functional Methods *J. Chem. Theory Comput.* 2017, 13, 515−524.